Case Studies in Chemical and Environmental Engineering 9 (2024) 100680

Contents lists available at ScienceDirect

Case Studies in Chemical and Environmental Engineering

journal homepage: www.sciencedirect.com/journal/case-studies-in-chemical-and-environmental-engineering

Case Report

# Spatial mapping and analysis of forest fire risk areas in Sri Lanka – Understanding environmental significance

Randika K. Makumbura [a], Prasad Dissanayake [b], Miyuru B. Gunathilake [c,d], Namal Rathnayake [e], Komali Kantamaneni [f], Upaka Rathnayake [g,*]

[a] Water Resources Management and Soft Computing Research Laboratory, Millennium City, Athurugiriya, 10150, Sri Lanka
[b] Faculty of Engineering and Information Sciences, University of Wollongong, Northfields Ave, Wollongong, NSW, 2522, Australia
[c] Hydrology and Aquatic Environment, Division of Environmental and Natural Resources, Norwegian Institute of Bioeconomy and Research, 1431, Ås, Norway
[d] Water, Energy and Environmental Engineering Research Unit, Faculty of Technology, University of Oulu, 90014, Oulu, Finland
[e] Department of Civil Engineering, Faculty of Engineering, The University of Tokyo, 1 Chome-1-1 Yayoi, Bunkyo City, Tokyo, 113-8656, Japan
[f] School of Engineering, University of Central Lancashire, Preston, PR1 2HE, United Kingdom
[g] Department of Civil Engineering and Construction, Faculty of Engineering and Design, Atlantic Technological University, F91 YW50, Sligo, Ireland

ARTICLE INFO

*Keywords:*
Forest fire index (FFI)
Geographic information system (GIS)
MODIS hotspot
Kernel density estimation (KDE)
Remote sensing top of form

ABSTRACT

This study presents the first attempt in Sri Lanka to generate a forest fire risk map covering the entire country using a GIS-based forest fire index (FFI) model. The model utilized seven parameters: land use, temperature, slope, proximity to roads and settlements, elevation, and aspect. All these parameters were derived using GIS techniques with ArcGIS10.4 and QGIS3.16. Data from Remote Sensing sources, particularly the MODIS hotspot real-world dataset, were employed to gather fire count information for the year 2020. Validation was conducted through the merging hotspot technique and kernel density estimation (KDE). The research findings highlight the districts in the Central and Uva provinces, such as NuwaraEliya (10.3 $km^2$), Kandy (2.74 $km^2$), and Badulla (10.41 $km^2$), as having a "very low risk" of forest fire potential. Conversely, districts like Hambanthota (0.1 $km^2$), Kaluthara (0.04 $km^2$), and Kurunegala (0.2 $km^2$) exhibit a "very high risk" of forest fire potential, although it is negligible compared country's total area. Overall, the study suggests that Sri Lanka is not currently facing a significant threat of forest fires and is a "medium risk" of forest fires as 49.49% of land falls under this category. These results are of immense value to relevant authorities, including the Ministry of Wildlife and Forest Resources Conservation, in formulating effective strategies to manage and mitigate forest fire risks in the country.

## 1. Introduction

Forests are essential natural resources and critical in maintaining climate balance and preserving soil, water, and biodiversity [1]. Food and Agriculture Organization's (FAO) report on the world's forests indicated forests cover 31% of the Earth's land surface (4.06 billion ha in 2020). However, the area is decreasing, with 420 million ha of forest lost between 1990 and 2020 due to various destructive factors [2]. These include deforestation, climate conditions (droughts, etc.), infectious diseases, and unplanned urbanization. However, forest fires have been identified as one of the primary causes of this forest shrinkage [3,4].

Forest fires significantly threaten wildlife and plants and result in irreversible ecological damage [5–8]. The adverse consequences of forest fires involve changed land use, greenhouse gas emissions, and massive food wastage around various areas of the ecosystem [8–10]. The trend and occurrence of forest fires have expanded significantly in numerous regions worldwide, causing significant concern [11–16]. Additionally, society is gradually becoming more conscious of how human interference with the ecosystem primarily results in natural disasters that endanger the health and well-being of humans [17,18].

Hence, it becomes paramount to raise awareness about fire hazard zones and educate the public so they can take necessary precautions proactively. Utilizing remote sensing (RS) and geographic information systems (GIS), forest fire risk zones can be accurately mapped and offers

* Corresponding author.
*E-mail addresses:* randikamk.96@gmail.com (R.K. Makumbura), pbgdk990@uowmail.edu.au (P. Dissanayake), miyuru.gunathilake@nibio.no (M.B. Gunathilake), namal@hydra.t.u-tokyo.ac.jp (N. Rathnayake), kkantamaneni@uclan.ac.uk (K. Kantamaneni), upaka.rathnayake@atu.ie, upakasanjeewa@gmail.com (U. Rathnayake).

https://doi.org/10.1016/j.cscee.2024.100680
Received 7 February 2024; Received in revised form 29 February 2024; Accepted 2 March 2024
Available online 4 March 2024

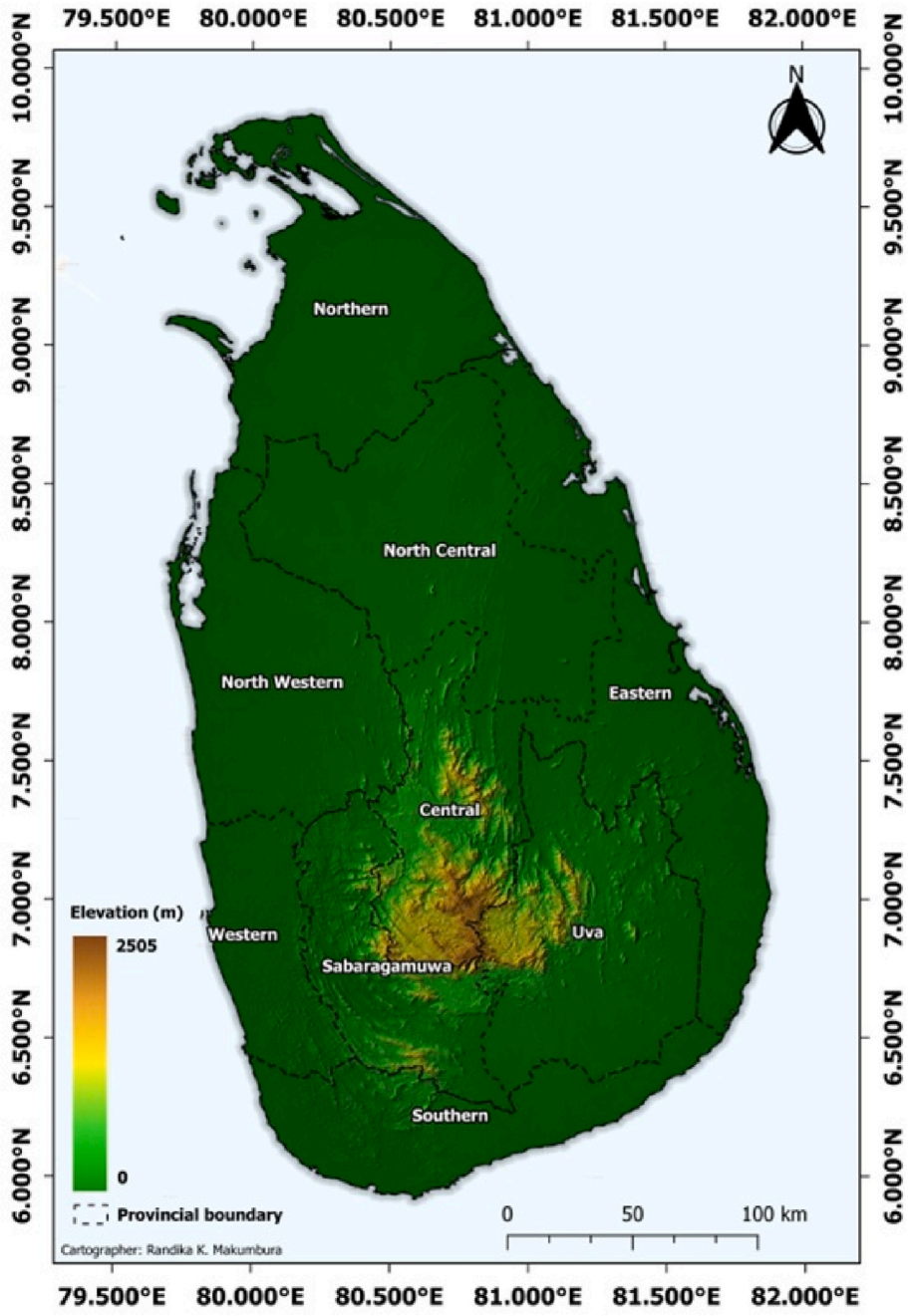


**Fig. 1.** Study area (Sri Lanka) with central provinces and spatial elevation variation (in m).

a vital platform for effective forest fire crisis management [19–22]. These technologies serve multiple functions, including information analysis, decision-making support, and data collection and storage, particularly in operational contexts where spatial decisions hold critical importance [23–25].

Many researchers worldwide have developed forest fire maps in recent years using RS and GIS techniques [1,26–29]. Jaiswal et al., 2002 [1] developed a forest fire risk map for the Gorna Sub watershed, located in Madhya Pradesh, India, by assigning subjective weights to the classes of all the layers according to their sensitivity to fire or their fire-inducing capability and found that almost 30% of the study area was predicted to be under very high and high-risk zones. Xu Dong. 2005 [6] used remote sensing and GIS in Baihe, Jilin Province, China, to create a map of possible wildfire zones. Moreover, Setiawan et al., 2004 [30] discovered and mapped peat swamp forest fire risk zones through GIS-grid-based and multi-criteria analysis in order to offer pertinent data for the Pekan District in the southern Pahang area of Malaysia.

Forest fires have become increasingly frequent in Sri Lanka in recent years, mainly due to human activities such as agricultural expansion, logging, and urbanization [31]. However, only a few studies have been conducted to identify forest fires' causes and impacts [32,33]. Sandamali & Chathuranga, 2021 [32] conducted a study to quantify burned severity of forest fire using Sentinel-2 remote sensing images covering the Ella Rock region in Sri Lanka. Sentinel-2 images served as the primary data source in that particular study, and remote sensing methods were used to analyze the QGIS open-source environment via the semi-automatic classification plugin. (SCP). Moreover, Basnayake et al., 2021 [33] developed a fire risk zone map covering the whole Belihuloya Mountain range in Sri Lanka, subjected to forest fires annually in the dry season. In order to facilitate that, a forest fire hazard zone mapping was

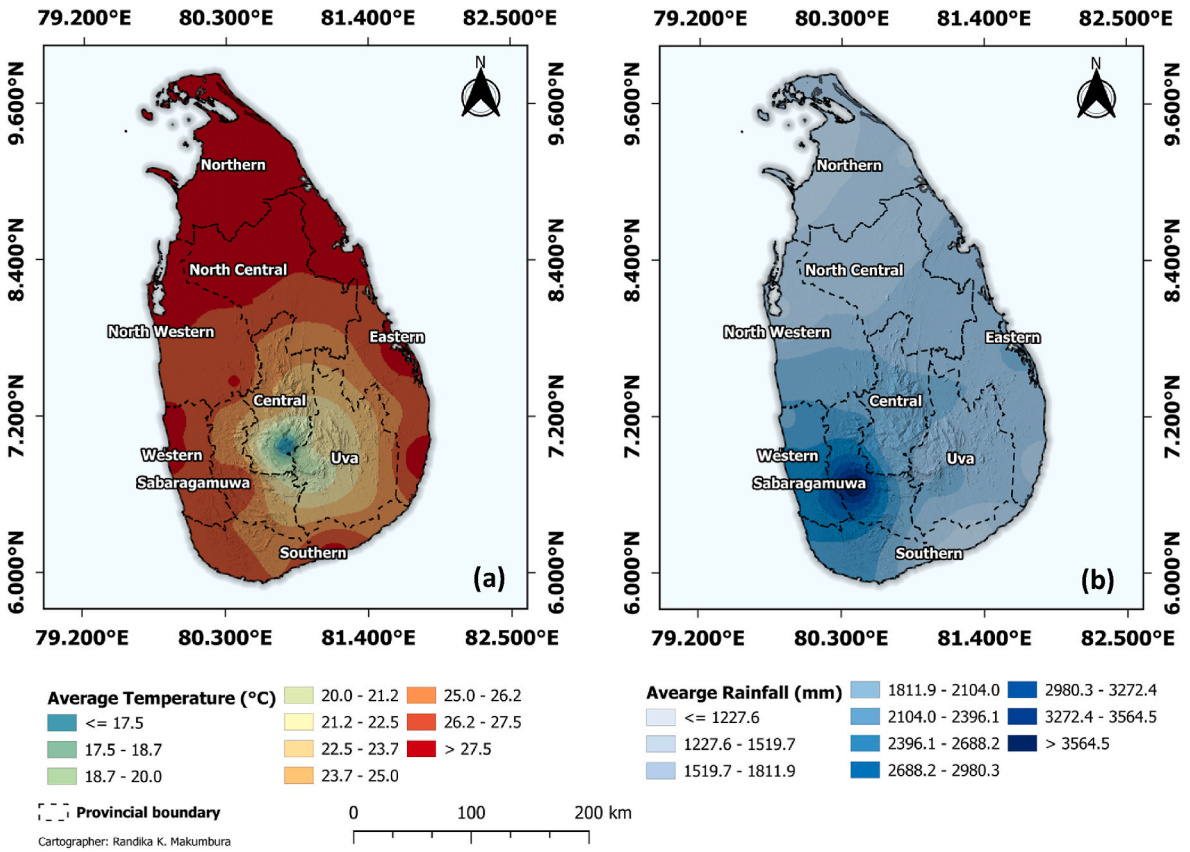


**Fig. 2.** Spatial variation of (a) annual mean temperature (in °C) and (b) annual rainfall (in mm) in Sri Lanka.

composed using GIS and remote sensing techniques. These research projects had been conducted for selective areas in Sri Lanka, but no research study has been executed so far with a fire risk mapping composed, covering the entire country.

In this study, a forest fire map was developed using remote sensing and GIS techniques to identify potential forest fire risk areas for 2020. According to the author's knowledge, this research represents the first-ever comprehensive remote sensing and GIS-based forest fire mapping study covering the entire country. The primary objective of the study is to draw the attention of relevant authorities, inspiring them to design more advanced real-time maps using the latest information, using this study as a baseline for forest fire risk mapping. Additionally, the insights gathered from this study shed light on the contributing factors to forest fire risks and risk areas, providing stakeholders with invaluable knowledge to formulate effective forest fire prevention and management strategies. By disseminating this valuable data, the public can become more aware of forest fire risk zones, encouraging proactive measures to protect the environment and communities from potential fire hazards.

## 2. Materials and methods

### 2.1. Study area

Sri Lanka (7.8731°N, 80.7718°E) (refer to Fig. 1), commonly named "Pearl Island" in the Indian Ocean, was selected for this study. Sri Lanka, an island country with an area of 65,525 km$^2$, is home to around 21,8 million citizens. Forest cover was about 25,600 km$^2$ in 2000 and gradually decreased to 22,490 km$^2$ by 2020, representing 34 % of the total land area [34,35]. Among the area's 2.04 million hectares of untouched forest, 0.7 million hectares of planted forests exist. Close canopy forests account for 1.58 million hectares, representing 23.9% of the total area of natural forests. The distribution of native forests is entirely random, with 86% located in dry and intermediate zones. The sparse and open forests comprise 90% of the country, while the closed canopy forests account for 85% [36]. Sri Lanka is endowed with a diverse range of forest types, comprising nine distinct categories. These forest types are as follows: montane forest, submontane forest, lowland rainforest, dry monsoon forest, moist monsoon forest, riverine dry forest, mangroves, sparse forest, and forest plantations excluding rubber [36].

The climate of Sri Lanka comprises four seasons, including first and second inter monsoons, southwest monsoon, and northeast monsoon. The two main monsoons, including southwest and northeast monsoons, typically occur between May, September, and December and February, respectively [37]. The western slopes of the central highlands experience the most annual precipitation, which varies from around 900 to over 5000 mm (Fig. 2 b), whereas the average temperature ranges between 16 °C and 27 °C (Fig. 2 a) in central highlands and the coastal belt respectively.

### 2.2. Forest fire influencing factors

The occurrence and spread of forest fires can be attributed to various factors, such as land use type, weather conditions, and terrain characteristics, among others. However, in this study, the authors have focused on the most common and widely used factors that influence forest fires, as described in previous studies [1,38,39]. Therefore, it is crucial to take these factors into consideration when developing a forest fire index or model.

#### 2.2.1. Topography

Topography is an essential physiographic factor, and its characteristics have an effect on forest survival following a wildfire [40]. In this study, we used a Shuttle Radar Topography Mission (SRTM) Digital Elevation Model (DEM) with a 30 m resolution to extract Sri Lanka's

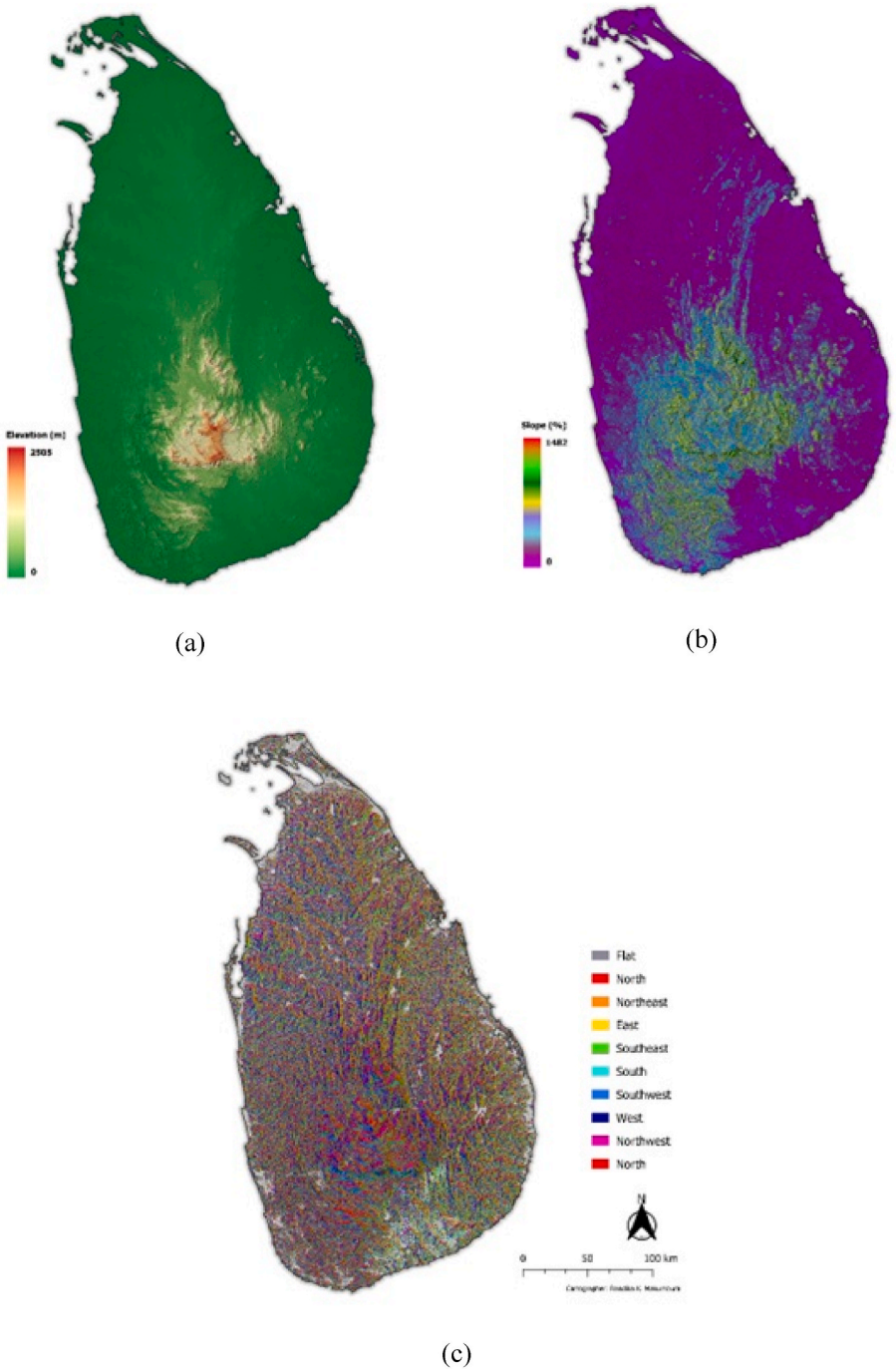


**Fig. 3.** Topographic characteristics of Sri Lanka, including (a) elevation (in meters), (b) slope (as a percentage of rise), and (c) aspect.

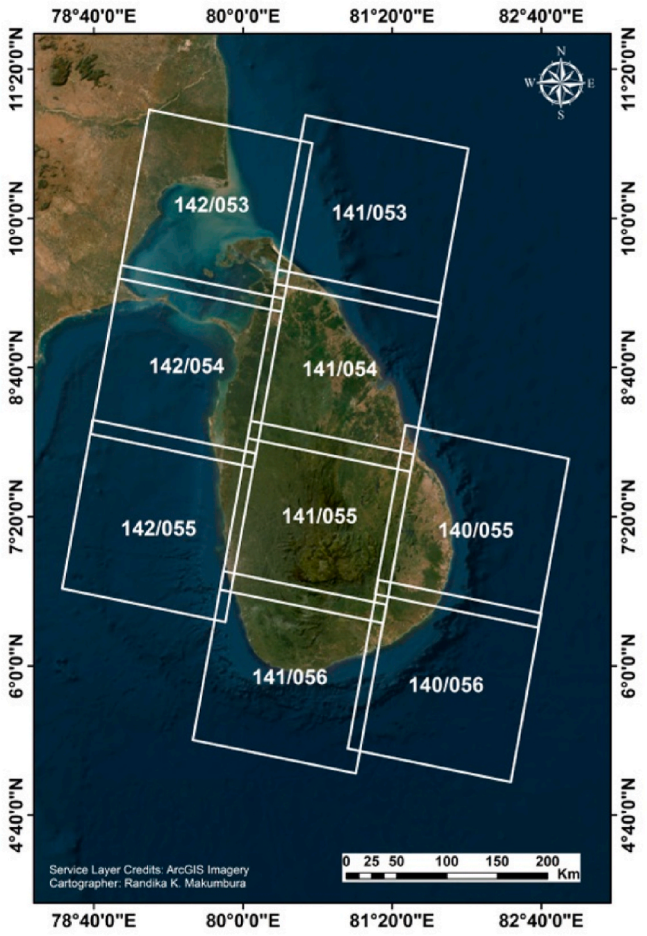


**Fig. 4.** Landsat 8 tiles arrangement for Sri Lanka (illustrated the path and row for each tile as per the USGS Earth Explorer).

**Table 1**
Data set information, Sensors, and Bands.

| Satellite | Sensor ID | Path/Row | Acquisition Date | Cloud Cover (%) |
|---|---|---|---|---|
| Landsat 8 | OLI/TIRS | 142/053 | 07-07-2020 | 0.7 |
| | | 142/054 | 07-07-2020 | 2.1 |
| | | 142/055 | 07-07-2020 | 1.9 |
| | | 141/053 | 04-10-2020 | 5 |
| | | 141/054 | 29-03-2021 | 0.4 |
| | | 141/055 | 13-07-2017 | 3 |
| | | 141/056 | 09-02-2021 | 2.7 |
| | | 140/055 | 03-03-2020 | 3.2 |
| | | 140/056 | 03-03-2020 | 0.6 |

topographic characteristics, including slope, aspect, and elevation (refer to Fig. 3). The points were extracted using ArcGIS 10.4.

### 2.2.2. Land use land cover (LULC)

*2.2.2.1. Landsat data.* The United States Geological Survey (USGS) Earth Explorer (available for free at https://earthexplorer.usgs.gov/) was used to acquire Landsat images of Sri Lanka. These Landsat images have a 30 m × 30 m resolution and are in raster format. Landsat 8 OLI remote sensing data was used to extract the images for the year 2020. Fig. 4 shows nine Landsat images encompassing Sri Lanka utilized in this study. These images were cloudless or had a cloud cover of less than 10%. However, only a small percentage of satellite images had cloud coverage exceeding 10%. To ensure accuracy, Landsat images from the most recent years with less than 10% cloud cover were employed in these instances (refer to Table 1). Therefore, this can be a potential limitation of this study.

*2.2.2.2. Classification of LULC.* High-resolution satellite imagery obtained from the Google Earth simulator was utilized in this study to map the land use classes. The classification process encompassed six distinct categories, namely water bodies, forests, bare lands, settlements, agriculture, and cloud cover. To achieve this classification, a nonparametric supervised method was employed, as depicted in Fig. 5. The USGS classification system guidelines were followed in establishing the land use classes [41]. The classification process was carried out using the ArcGIS 10.4.1 software application. Minimum training samples and pixel counts as per the standards [42] were assigned to each land use class during the classification process.

Accuracy assessment was conducted for land use classification, achieving an overall accuracy of 90% and a kappa coefficient (Eq (1)) of 88%. To evaluate the accuracy, 300-pixel points were overlaid using Google Earth, surpassing the minimum requirement of 50 sample points, as described by C. Schmidt and A. McCullum, 2018 [43]. KAPPA analysis provides a statistic called Khat (Eq (1)), which measures the accuracy of a LULC classification [44].

$$K = \frac{N\sum_{i=1}^{r} x_{ii} - \sum_{i=1}^{r}(x_{i+} \times x_{+i})}{N^2 - \sum_{i=1}^{r}(x_{i+} \times x_{+i})} \tag{1}$$

$N$ = total observations in the matrix
$r$ = rows and columns in the matrix
$x_{+i}$ = marginal total of column $i$
$x_{i+}$ = marginal total of row $i$
$x_{ii}$ = number of observations in row $i$ and column $i$

### 2.2.3. Land surface temperature (LST)

Landsat 8 satellite images used for LULC classification were used for Land Surface Temperature (LST) analysis, and the thermal band (band 10) was utilized to retrieve LST—first, digital number (DN) values were converted to absolute radiance values using Equation (2) [45].

$$L_\lambda = M_L \times Q_{cal} + A_L \tag{2}$$

$L_\lambda$ = Spectral radiance $(watts/(m^2 \times sr \times \mu m))$.
$M_L$ = Radiance multiplicative scaling factor for the band
$Q_{cal}$ = Level 1 pixel value in DN
$A_L$ = Radiance additive scaling factor for the band

After the conversion of DN values to the absolute radiance, radiance luminance to satellite brightness temperature $T_B(^\circ C)$ conversion was performed using Equation (3).

$$T_B(^\circ C) = \frac{k_2}{\ln\left(\frac{k_1}{L_\lambda} + 1\right)} - 273.15 \tag{3}$$

$k_1 = 774.8853\ watts/m^2 \times sr \times \mu m.$
$k_2 = 1321.0789$ K

Finally, emissivity-corrected LST was calculated (refer to Fig. 6) using the following Equation [46].

$$LST(^\circ C) = \frac{T_B}{1 + \left(\lambda \times \frac{T_B}{\rho}\right) ln\ \varepsilon} \tag{4}$$

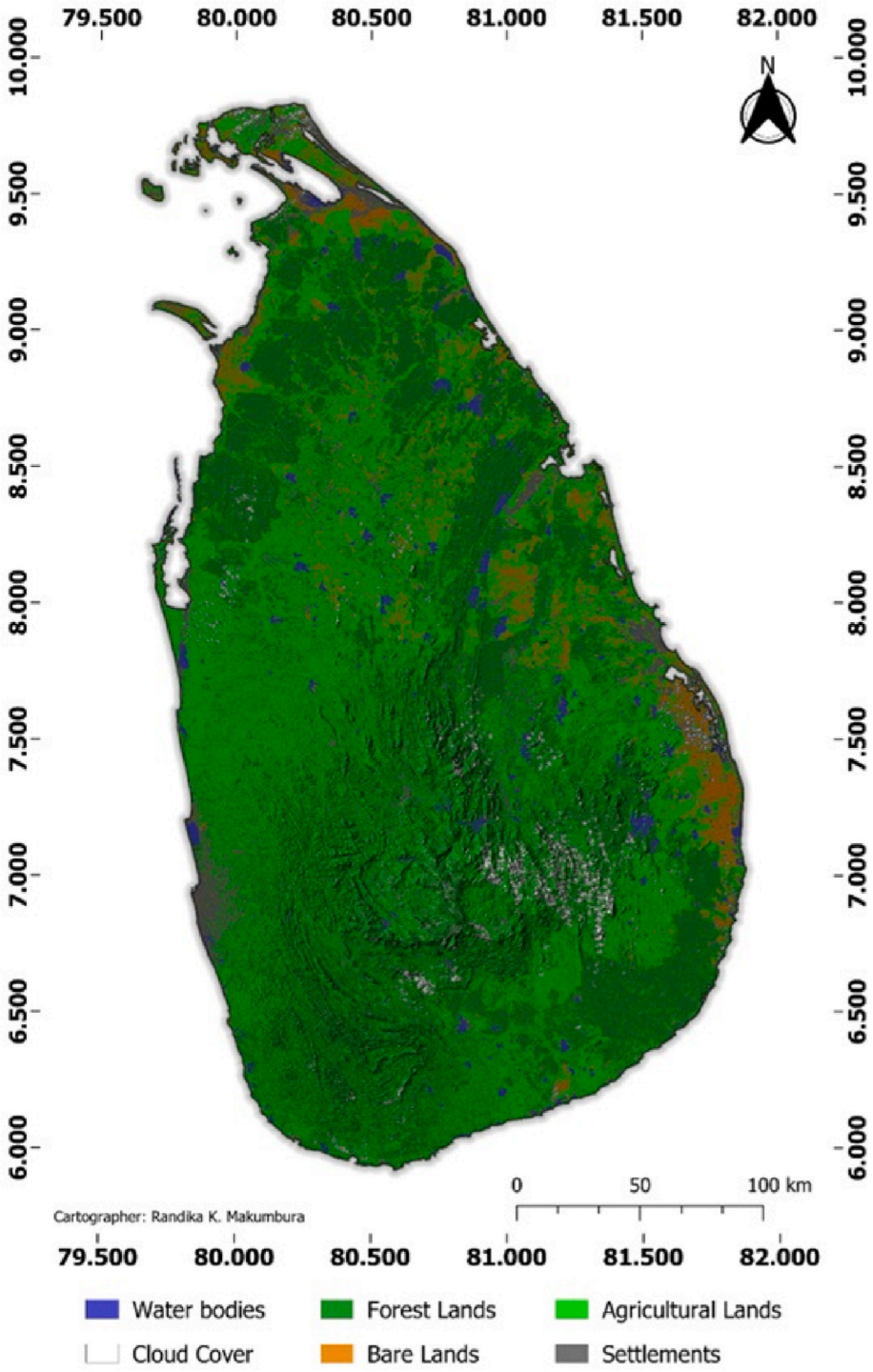


**Fig. 5.** Supervised Land Use Land Cover (LULC) classification map for five land use classes (excluding cloud cover) in 2020.

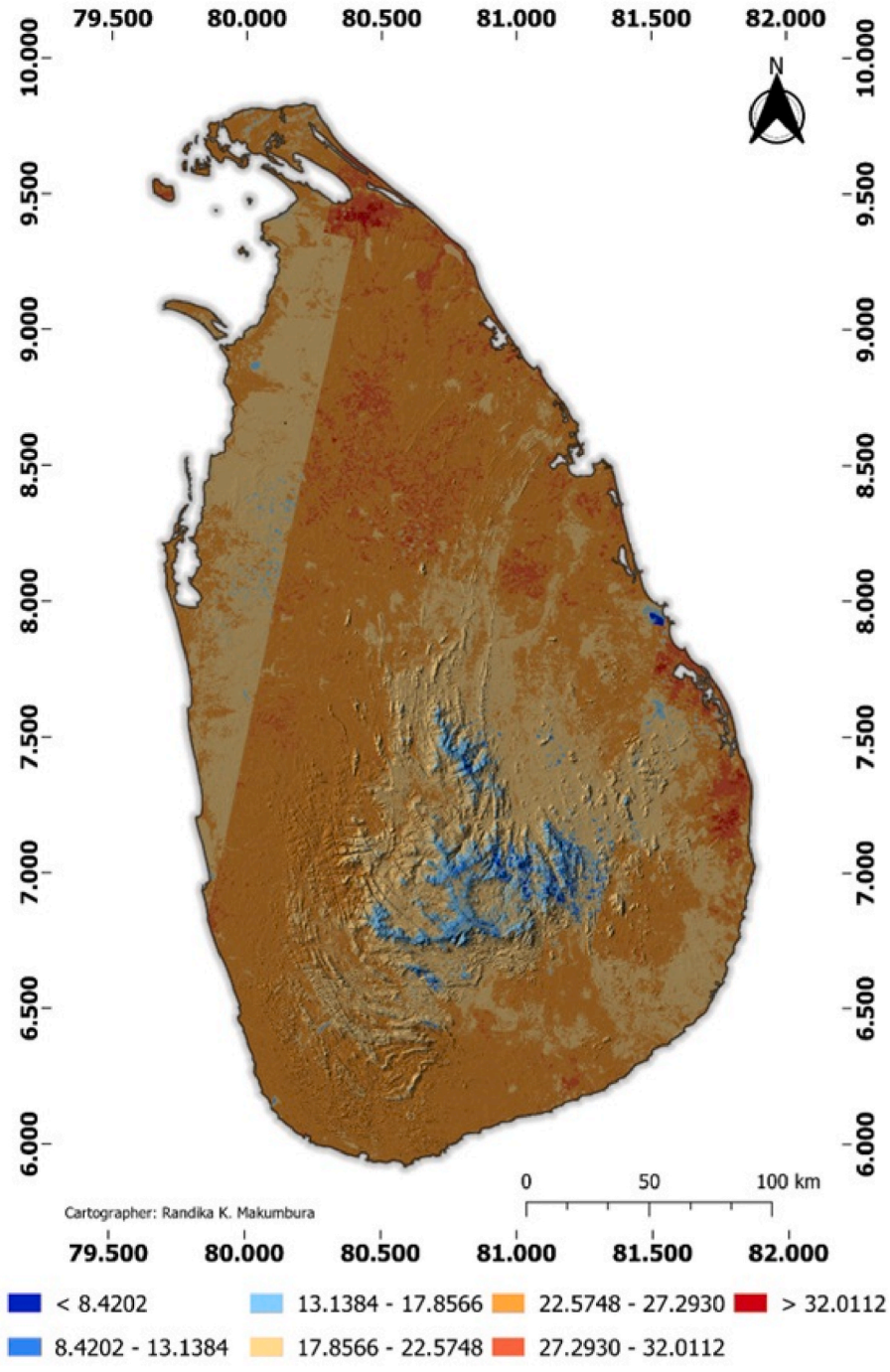


**Fig. 6.** Spatial variation of Land Surface Temperature (LST) for Sri Lanka in 2020.

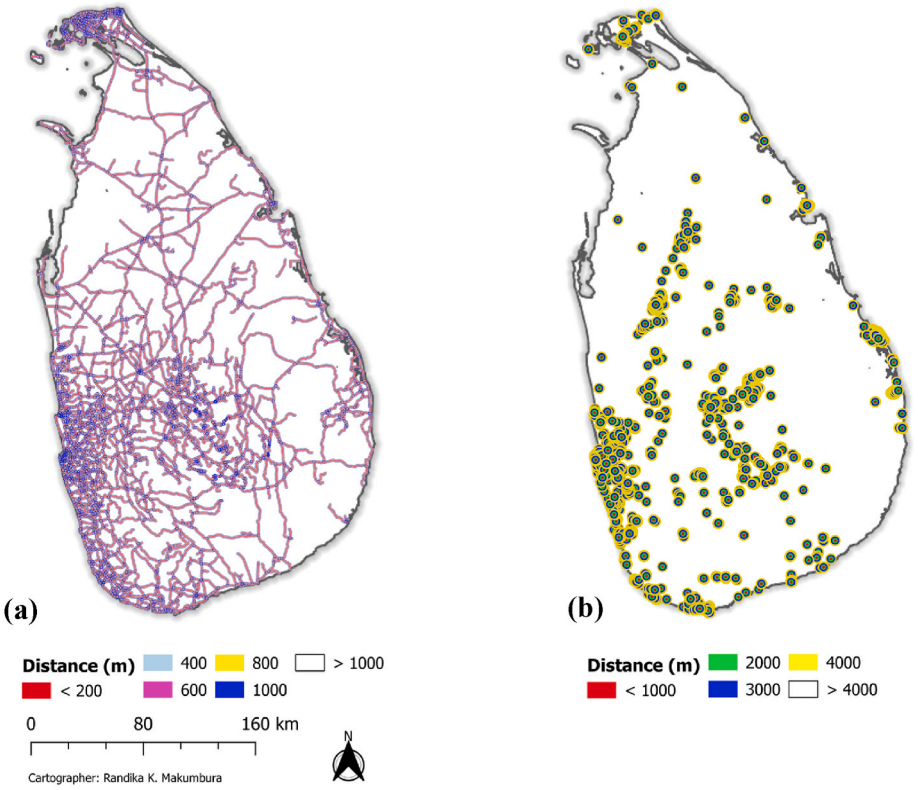


**Fig. 7.** Distribution of the (a) main road network and (b) settlements (spatial distribution of main buildings such as hotels, hospitals, etc) in Sri Lanka.

$T_B$ = Landsat-8 Band 10 brightness temperature
λ = wavelength of emitted radiance (λ = 10.8 μm)
$\rho = h \times c/\sigma$ ($1.438 \times 10^{-2}$ mK)
h = $6.626 \times 10^{-34}$ Js - Planck's constant
σ = $1.38 \times 10^{-23}$ J/K - Boltzmann constant
c = $2.998 \times 10^{8}$ m/s - velocity of light
$\varepsilon$ = land surface emissivity (refer to Equation (5)) [47,48]

$$\varepsilon = mP_v + n \tag{5}$$

$m = (\varepsilon_v - \varepsilon_s) - (1 - \varepsilon_s)F\varepsilon_v$.
$n = \varepsilon_s + (1 - \varepsilon_s)F\varepsilon_v$.
$\varepsilon_v$ = vegetation emissivity
$\varepsilon_s$ = soil emissivity

Following equations were used to obtain the $P_v$ value in Equation (5) [49].

$$NDVI = \frac{NIR - Red}{NIR + Red} \tag{6}$$

$$P_v = \left(\frac{NDVI - NDVI_{min}}{NDVI_{max} - NDVI_{min}}\right)^2 \tag{7}$$

where NDVI is the Normalized Difference Vegetation Index.

#### 2.2.4. Proximity to roads and settlements

Roads and settlements are one of the primary contributors to accidental or human-caused forest fires, where most human activities, such as haphazardly thrown matches and cigarette ends, occur. Therefore, forests near roads and settlements are more prone to fire and at a greater risk [27]. Thus, the authors selected the main road network in Sri Lanka for this study, as shown in Fig. 7 a, and buffered it into six categories (0–200 m, 200–400 m, 400–600 m, 600–800 m, 800–1000 m, and greater than 1000 m) using the multiple ring tool in ArcGIS.

Further, obtaining settlement data for Sri Lanka was also one of the most challenging aspects of this research. This large study area made it more difficult to map every homestead and nearly impossible without a comprehensive survey data set. Therefore, the authors have selected only the significant buildings (hotels, hospitals, schools, etc.) covering the country, as shown in Fig. 7 b. This will be a potential limitation of this study. Then the selected point feature was buffered into five groups (0–1000 m, 1000–2000 m, 2000–3000 m, 3000–4000 m, and greater than 4000 m) utilizing a constant distance multiple ring buffer tool in QGIS 3.16.

### 2.3. FFI model validation data

The Moderate Resolution Imaging Spectroradiometer (MODIS) is a sophisticated remote sensing instrument capable of data collection across multiple time frames. With its near-real-time data availability, MODIS is a valuable tool for monitoring active fires and burnt areas, offering the potential to improve forest fire management during the fire season [50,51]. As one of the Earth Observation System's (EOS) sensors, MODIS contains great potential for enhancing forest fire monitoring and control strategies.

In this study, data for the year 2020 (a total of 735 fire counts) (refer to Fig. 8) were acquired from the Fire Information for Resources Management System (https://firms.modaps.eosdis.nasa.gov/) - a readily available source of fire data. The primary purpose was to validate the results of the FFI model at a 1 km resolution. Notably, the Detection confidence, which estimates the confidence level of fire detection and ranges from 0% to 100%, allows the assignment of fire pixels into one of three classes: low-confidence fire, nominal-confidence fire, or high-confidence fire. Previous research by Giglio et al. (2003) [52] suggests that a threshold above 30% yields better accuracy in this classification process. However, it is essential to acknowledge that this study relies solely on the provided data and cannot independently validate them due

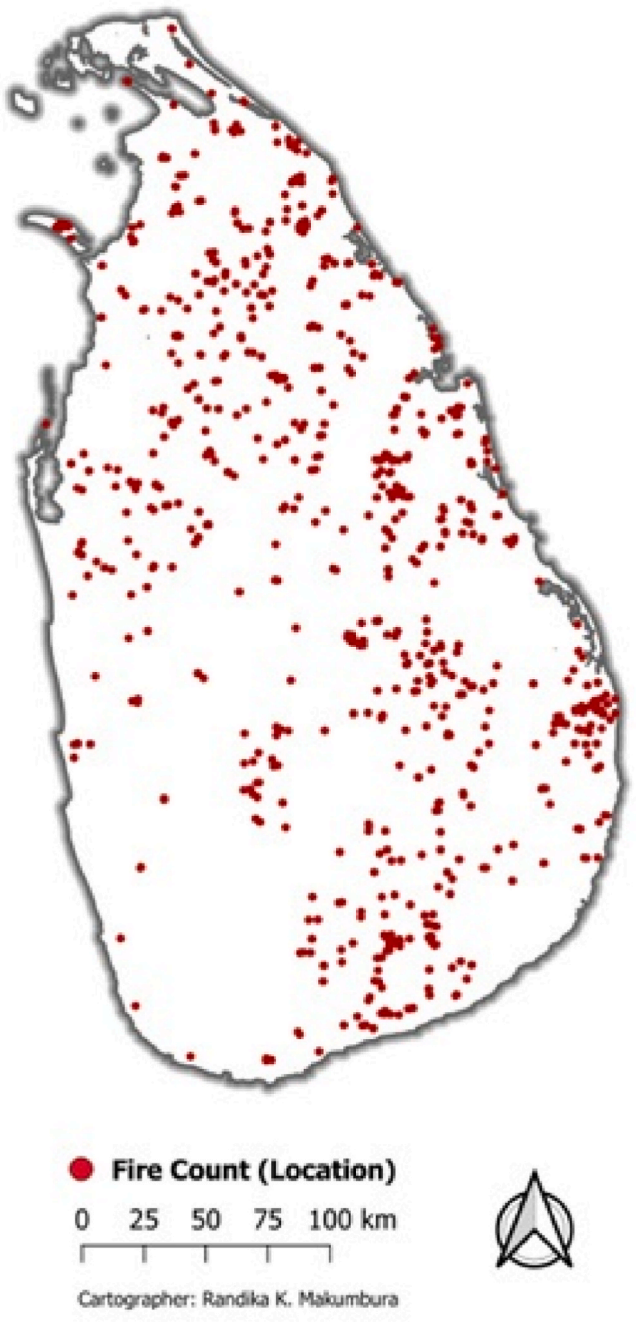


**Fig. 8.** Spatial distribution of MODIS fire counts (locations) across Sri Lanka in 2020 obtained from FIRMS.

to the absence of freely available fire databases in Sri Lanka. As a result, this uncertainty poses a limitation on the study. Nevertheless, it is worth noting that numerous other studies have successfully validated MODIS data and achieved satisfactory accuracy [53].

### 2.4. Development of the forest fire risk (FFR) map

The Forest Fire Risk areas were delineated using a Forest Fire Index (FFI) model (Equation (8)), which was developed by assigning weight factors to each input data. This approach was adopted to minimize potential model errors and derive meaningful conclusions based on relevant literature [1,27,50]. The ranking of input variables based on their fire hazard sensitivity, ranging from 1 (very high risk) to 5 (very low risk), is presented in Table 2. Subsequently, each variable's weightage was determined, and all layers were superimposed using ArcGIS to generate the Forest Fire Risk (FFR) map. The overall procedure for developing the forest fire risk map is illustrated in Fig. 9.

**Table 2**
Classification of factors and the corresponding weight assignment to the forest fire risk model.

| Factor | Weight (%) | Category | Value assigned | Ranking |
|---|---|---|---|---|
| Land Use Land Cover (LULC) | 40 | Vegetation | 1 | Very High |
| | | Settlements | 3 | Medium |
| | | Agriculture | 4 | Low |
| | | Bare Lands | 5 | Very Low |
| Land Surface Temperature (LST) (°C) | 20 | >35 | 1 | Very High |
| | | 30–35 | 2 | High |
| | | 25–30 | 3 | Medium |
| | | 20–25 | 4 | Low |
| | | <20 | 5 | Very Low |
| Slope (%) | 10 | <5 | 1 | Very High |
| | | 5–15 | 2 | High |
| | | 15–25 | 3 | Medium |
| | | 25–35 | 4 | Low |
| | | >35 | 5 | Very Low |
| Distance to road (m) | 10 | <200 | 1 | Very High |
| | | 200–400 | 2 | High |
| | | 400–600 | 3 | Medium |
| | | 600–800 | 4 | Low |
| | | 800–1000 | 5 | Very Low |
| | | >1000 | 5 | Very Low |
| Proximity to settlements (m) | 10 | <1000 | 1 | Very High |
| | | 1000–2000 | 2 | High |
| | | 2000–3000 | 3 | Medium |
| | | 3000–4000 | 4 | Low |
| | | >4000 | 5 | Very Low |
| Elevation (m) | 5 | <500 | 1 | Very High |
| | | 500–600 | 2 | High |
| | | 600–700 | 3 | Medium |
| | | 700–800 | 4 | Low |
| | | >800 | 5 | Very Low |
| Aspect | 5 | South | 1 | Very High |
| | | South West | 1 | Very High |
| | | South East | 2 | High |
| | | West | 3 | Medium |
| | | East | 3 | Medium |
| | | North West | 4 | Low |
| | | North East | 4 | Low |
| | | North | 5 | Very Low |

$$FFI = 40\%\ LULC + 20\%\ LST + 10\%\ S + 10\%\ DR + 10\%\ PS + 5\%\ A + 5\%\ E \quad (8)$$

Where LULC, LST, and S represent land use land cover, land surface temperature, and terrain slope, respectively, DR and PS indicate the distance to roads and proximity to settlements. The aspect is A, and the elevation is E.

#### 2.4.1. Forest fire index (FFI) model validation

The FFI model was validated using MODIS hotspot data taken as the real-world dataset. After deriving the FFI model from seven selected

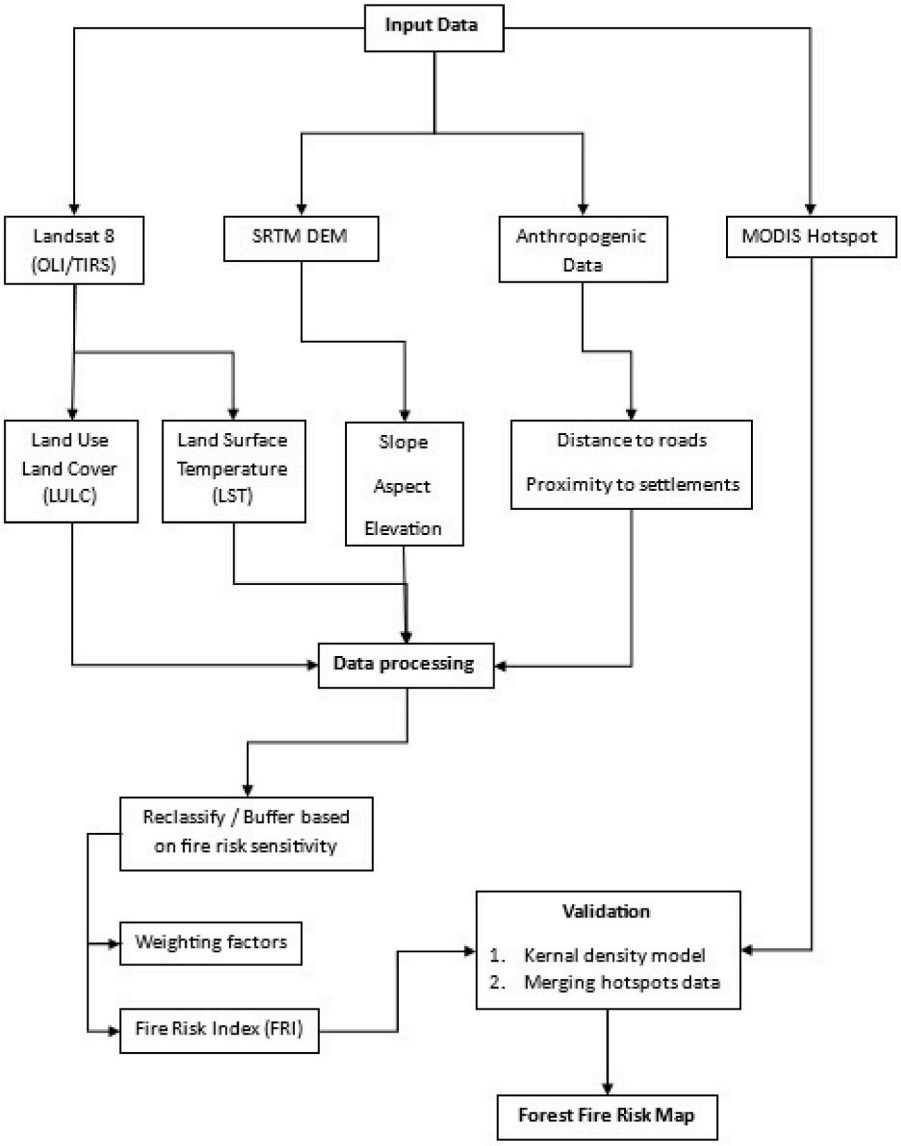


**Fig. 9.** Methodological framework for the development of the FFR map in Sri Lanka.

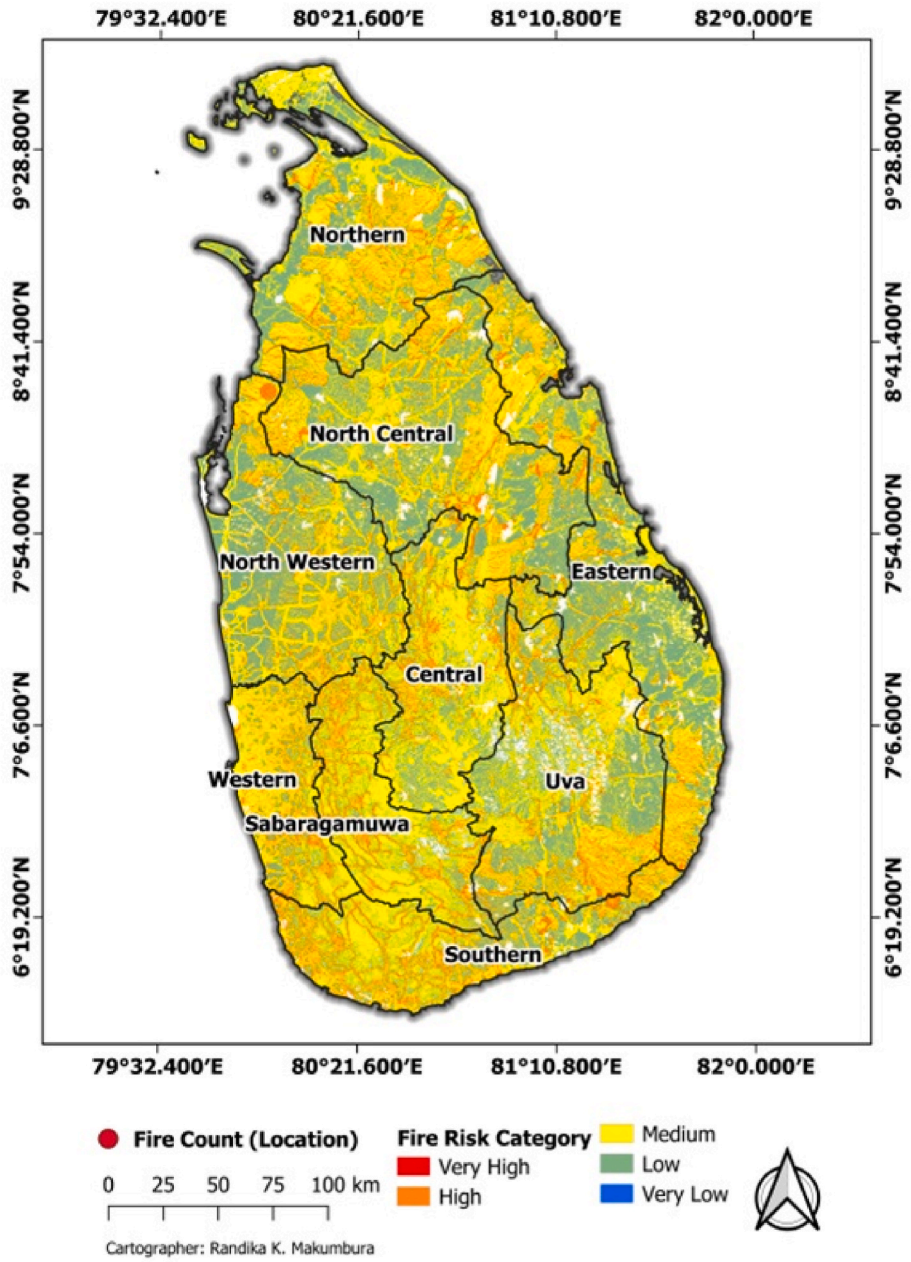


**Fig. 10.** The forest fire risk map of Sri Lanka created using the FFI for the year 2020.

independent variables, archive fire counts were superimposed on the FFI map in order to compare the actual data with the obtained results. Given that the MODIS detection confidence is estimated within a range of 0%–100%, it is utilized to categorize fire pixels into one of three classes: low-confidence fire, nominal-confidence fire, or high-confidence fire. Therefore, in this study, the authors considered the very high-risk, high-risk, and medium-risk areas identified in the FFI map as potential fire-risk locations. These areas were then compared with the data obtained from the MODIS hotspot.

Then, Kernel density estimation (KDE) was conducted to compare the obtained values with real-world data. The primary objective of KDE (Kernel Density Estimation) is to create a continuous density surface of point events across space. This is achieved by estimating the event intensity as density [54].

## 3. Results and discussion

### 3.1. Forest fire index model

The Forest Fire Index (FFI) model was developed using seven independent parameters, and based on this model, a forest fire map was generated (refer to Fig. 10). Notably, the map reveals that “very high risk" forest fire areas are minimal compared to other risk categories, indicating a relatively low significant impact of very high-risk areas on the country, as suggested by the obtained results. A noteworthy finding is the gradual decrease in risk observed in the central province, which can be attributed to factors such as high altitude and lower temperatures.

The Sinharaja forest within Sabaragamu and Southern provinces is particularly intriguing as it is the country’s last large, viable area of virgin primary tropical rainforest. This forest, encircled by three districts (Rathnapura, Matara, and Galle), is predominantly classified under the

**Table 3**
Districts with potential risk areas under each risk category.

| District | The area under each risk category (in $km^2$) | | | | |
|---|---|---|---|---|---|
| | Very High | High | Medium | Low | Very Low |
| Ampara | 0.00 | 528.14 | 1757.36 | 2026.43 | 0.32 |
| Anuradhapura | 0.02 | 794.67 | 3255.20 | 2919.61 | 0.02 |
| Badulla | 0.00 | 249.59 | 1346.99 | 1021.94 | **10.41** |
| Batticaloa | 0.00 | 155.88 | 973.10 | 1215.70 | 0.17 |
| Colombo | 0.03 | 120.27 | 455.39 | 99.08 | 0.00 |
| Galle | 0.02 | 386.48 | 858.09 | 338.31 | 0.00 |
| Gampaha | 0.07 | 270.05 | 825.60 | 283.03 | 0.00 |
| Hambantota | **0.10** | 562.59 | 1102.88 | 874.33 | 0.00 |
| Jaffna | 0.00 | 4.64 | 585.18 | 322.45 | 0.00 |
| Kalutara | **0.04** | 385.42 | 883.76 | 366.47 | 0.01 |
| Kandy | 0.00 | 297.58 | 1062.80 | 520.91 | **2.74** |
| Kegalle | 0.01 | 323.39 | 936.94 | 399.58 | 0.31 |
| Kilinochchi | 0.00 | 76.99 | 611.04 | 573.95 | 0.00 |
| Kurunegala | **0.20** | 634.07 | 2145.02 | 2073.76 | 0.08 |
| Mannar | 0.00 | 242.26 | 972.31 | 757.37 | 0.00 |
| Matale | 0.00 | 296.55 | 1157.13 | 571.50 | 2.50 |
| Matara | 0.01 | 254.12 | 727.72 | 295.45 | 0.01 |
| Moneragala | 0.02 | 817.63 | 2553.62 | 2067.06 | 1.57 |
| Mullaitivu | 0.00 | 465.09 | 1240.97 | 734.82 | 0.00 |
| Nuwara Eliya | 0.00 | 71.91 | 1039.61 | 528.98 | **10.30** |
| Polonnaruwa | 0.00 | 559.01 | 1420.20 | 1347.04 | 0.04 |
| Puttalam | 0.00 | 341.29 | 1109.40 | 1541.09 | 0.00 |
| Ratnapura | 0.00 | 515.35 | 1914.35 | 775.41 | 2.33 |
| Trincomalee | 0.00 | 366.52 | 1328.88 | 842.93 | 0.00 |
| Vavuniya | 0.00 | 400.95 | 1019.75 | 567.53 | 0.00 |

“medium risk" to “low-risk" categories. These three districts show a substantial presence of “medium risk" and “low risk" areas compared to other risk categories. Surprisingly, most forested areas fall into one of the risk categories (very high, high, and medium) in low-altitude regions with elevated temperatures. Curiously, the settlements and roads in these areas seem to have minimal impact on the likelihood of fire occurrence.

Based on the data presented in Table 3, a clear pattern emerges, indicating that districts in the central and Uva provinces, such as Nuwara Eliya (10.3 $km^2$), Kandy (2.74 $km^2$), and Badulla (10.41 $km^2$), are characterized by a very low risk of forest fires, likely due to the factors mentioned earlier. Additionally, these districts exhibit a higher

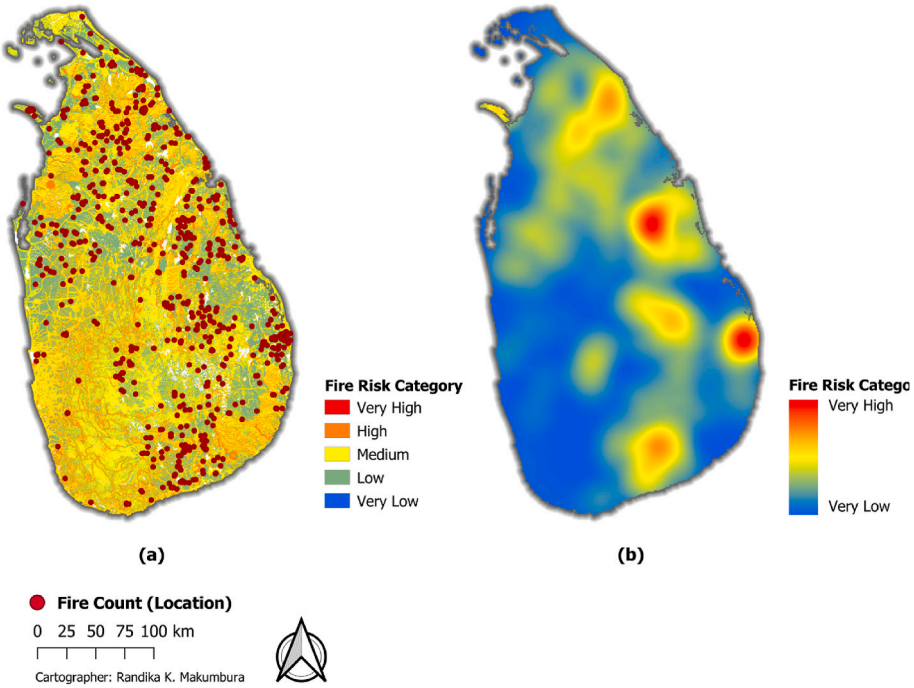


**Fig. 11.** (A) Merged MODIS hotspot data with FFI map, (b) Fire risk map produced using KDE method from MODIS hotspot data.

**Table 4**
Comparison of FFI and KDE risk areas falling under different risk categories.

| Risk category | Risk area from FFI (%) | Risk area from KDE (%) |
|---|---|---|
| Very high | 0 | 0.93 |
| High | 14.13 | 13.64 |
| Medium | 49.49 | 50.38 |
| Low | 36.33 | 31.32 |
| Very low | 0.05 | 3.73 |

proportion of “low-risk" and “medium-risk" areas compared to “very high-risk" and “high-risk" areas, suggesting a minimal likelihood of forest fires in these regions.

On the other hand, districts like Hambanthota (0.1 $km^2$), Kaluthara (0.04 $km^2$), and Kurunegala (0.2 $km^2$) are identified as “very high-risk" areas, although their total area is negligible when compared to Sri Lanka’s vast expanse of about 65,000 $km^2$. It is worth noting that Anuradhapura, the largest district in Sri Lanka, contains a significant portion of risk areas, with a prevalence of “medium risk" regions, primarily characterized by partial urbanization and a dry climate at low altitudes.

Based on the findings of this study, the forest fire risk areas in Sri Lanka were categorized as follows: very high risk (0.52 $km^2$, 0%), high risk (9120.44 $km^2$, 14.13%), medium risk (31,283.29 $km^2$, 49.49%), low risk (23,064.75 $km^2$, 36.33%), and very low risk (30.81 $km^2$, 3.73%). Consequently, this study classifies Sri Lanka as a country with a medium forest fire risk due to the predominant coverage of medium-risk areas, comprising approximately 49.49% of the total land area.

### 3.2. FFI model validation

A total of 735 fire counts were obtained for 2020 from the MODIS hotspot real-world dataset. These points were overlaid on the FFI map (refer to Fig. 11 a), and the results were extracted to facilitate comparison. Among the 735 fire counts, 468 points (63.58%) were identified as locations indicative of forest fire risk compared to the FFI map generated using the FFI model.

Then the KDE method was utilized to examine the forest fire areas that fall under each category (refer to Fig. 11 b) as it works as an appropriate development of a decision support system, as this method has been used as a tool for validation technique for forest fire risk map [55]. As shown in Table 4, the percentage of risk areas in the high-risk, medium-risk, and low-risk categories is almost identical for both the FFI model and KDE, suggesting that the FFI model exhibits good accuracy in conducting the analysis. However, there is a slight disparity in the very high-risk and very low-risk categories, which can be attributed to the uncertainties associated with the data used by the authors to develop the model.

## 4. Conclusions

This study’s primary objective is to map the fire risk areas for 2020 in Sri Lanka by employing a forest fire index model developed using seven independent parameters, including land use, temperature, slope, proximity to roads and settlements, elevation, and aspect. All these data were derived using GIS techniques with ArcGIS 10.4 and QGIS 3.16, as illustrated in the materials and methods section. The validation of the results involved utilizing MODIS hotspot data through a kernel density model and merging hotspot data. The study’s key findings emphasize that the districts within the Central and Uva provinces, such as Nuwara Eliya, Kandy, and Badulla, are characterized by a “very low risk" forest fire potential. Conversely, districts like Hambanthota, Kaluthara, and Kurunegala exhibit a “very high risk" of forest fire potential, although this risk remains minimal compared to the total country’s area. An in-depth district-wise analysis has been conducted (refer to Table 3), presenting relevant risk areas to readers and relevant authorities to guide further studies based on the outcomes generated in this research.

Overall, the findings of this study suggest that Sri Lanka is not currently facing a significant threat of forest fires and remains in the “medium risk" category. As the study introduces GIS-based forest fire mapping to the Sri Lankan context and lays the groundwork, it opens avenues for further enhancement. Given the strong relationship between the model and forest fires with monsoon patterns and wind patterns, future researchers and authorities can delve into different monsoons (southwest and northeast) to analyze the distribution of forest fire risk

across Sri Lanka. Such investigations will help reduce uncertainties in the model and yield more accurate results. Hence, the Ministry of Wildlife and Forest Resources Conservation and other relevant authorities can benefit from this knowledge to formulate effective strategies for forest fire management and conservation efforts, safeguarding the country's precious natural resources.

## Funding

This research received no external funding.

## CRediT authorship contribution statement

**Randika K. Makumbura:** Writing – original draft, Software, Resources, Methodology, Investigation, Formal analysis, Data curation. **Prasad Dissanayake:** Formal analysis, Data curation. **Miyuru B. Gunathilake:** Validation. **Namal Rathnayake:** Visualization. **Komali Kantamaneni:** Writing – review & editing. **Upaka Rathnayake:** Writing – review & editing, Supervision, Project administration, Conceptualization.

## Declaration of competing interest

The authors declare that they have no known competing financial interests or personal relationships that could have appeared to influence the work reported in this paper.

## Data availability

Data will be made available on request.

## References

[1] R.K. Jaiswal, S. Mukherjee, K.D. Raju, R. Saxena, Forest fire risk zone mapping from satellite imagery and GIS, Int. J. Appl. Earth Obs. Geoinf. 4 (1) (2002) 1–10.
[2] FAO, The state of the world's forests 2020 Available at: https://www.fao.org/state-of-forests/en/, 2023. (Accessed 23 April 2023).
[3] C. Gai, W. Weng, H. Yuan, GIS-based forest fire risk assessment and mapping, in: 2011 Fourth International Joint Conference on Computational Sciences and Optimization, IEEE, 2011, April, pp. 1240–1244.
[4] M. Bonazountas, D. Kallidromitou, P.A. Kassomenos, N. Passas, Forest fire risk analysis, Human and Ecological Risk Assessment 11 (3) (2005) 617–626.
[5] S. Aleemahmoodi Sarab, J. Feghhi, A. Danehkar, P. Attarod, Effects of dereference evapotranspiration and relative humidity on forest fire occurrences in Zagros Forests, west of Iran (Case study: khouzestan province), Iranian Journal of Forest and Range Protection Research 12 (2) (2014) 79–86.
[6] X.U. Dong, D.A.I. Li-min, S. Guo-fan, T. Lei, W. Hui, Forest fire risk zone mapping from satellite images and GIS for Baihe Forestry Bureau, Jilin, China, J. For. Res. 16 (3) (2005) 169–174.
[7] T. Mirdeilami, S.H. Shataee, M.R. Kavoosi, Forest Fire Risk Zone Mapping in the Golestan National Park Using Regression Logistic Method, 2015.
[8] D. Vakalis, H. Sarimveis, C. Kiranoudis, A. Alexandridis, G. Bafas, A GIS based operational system for wildland fire crisis management I. Mathematical modelling and simulation, Appl. Math. Model. 28 (4) (2004) 389–410.
[9] A. Alexandridis, D. Vakalis, C.I. Siettos, G.V. Bafas, A cellular automata model for forest fire spread prediction: the case of the wildfire that swept through Spetses Island in 1990, Appl. Math. Comput. 204 (1) (2008) 191–201.
[10] H. Faramarzi, S.M. Hosseini, M. Gholamalifard, Fire hazard zoning in national golestan park using logistic regression and GIS, Journal of Geography and Environmental Hazards 3 (2) (2014) 73–90.
[11] J.P. Argañaraz, G.G. Pizarro, M. Zak, M.A. Landi, L.M. Bellis, Human and biophysical drivers of fires in Semiarid Chaco mountains of Central Argentina, Sci. Total Environ. 520 (2015) 1–12.
[12] A. Arpaci, B. Malowerschnig, O. Sass, H. Vacik, Using multi variate data mining techniques for estimating fire susceptibility of Tyrolean forests, Appl. Geogr. 53 (2014) 258–270.
[13] D.T. Bui, Q.T. Bui, Q.P. Nguyen, B. Pradhan, H. Nampak, P.T. Trinh, A hybrid artificial intelligence approach using GIS-based neural-fuzzy inference system and particle swarm optimization for forest fire susceptibility modeling at a tropical area, Agric. For. Meteorol. 233 (2017) 32–44.
[14] J.S. Littell, D.L. Peterson, K.L. Riley, Y. Liu, C.H. Luce, A review of the relationships between drought and forest fire in the United States, Global Change Biol. 22 (7) (2016) 2353–2369.
[15] R. Mavsar, A.G. Cabán, E. Varela, The state of development of fire management decision support systems in America and Europe, For. Pol. Econ. 29 (2013) 45–55.
[16] M.A. Moritz, M.A. Parisien, E. Batllori, M.A. Krawchuk, J. Van Dorn, D.J. Ganz, K. Hayhoe, Climate change and disruptions to global fire activity, Ecosphere 3 (6) (2012) 1–22.
[17] G.D. Bathrellos, H.D. Skilodimou, K. Chousianitis, A.M. Youssef, B. Pradhan, Suitability estimation for urban development using multi-hazard assessment map, Sci. Total Environ. 575 (2017) 119–134.
[18] H. Kordani, B. Chaplot, P.R. Dehkharghani, H.M. Azamathulla, People's participation in using treated wastewater as an approach for sustainability of ecosystem services, green spaces, and farmlands in peri-urban areas: the case study of Kalak-e Bala, Karaj, Iran, Water Supply 22 (4) (2022) 4571–4583.
[19] N. Lymberopoulos, C. Papadopoulos, E. Stefanakis, N. Pantalos, F. Lockwood, A GIS-based forest fire management information system, EARSeL Adv. Remote Sens. (1996) 68–75.
[20] G.L. Perry, A.D. Sparrow, I.F. Owens, A GIS-supported model for the simulation of the spatial structure of wildland fire, Cass Basin, New Zealand, J. Appl. Ecol. 36 (4) (1999) 502–518.
[21] S. Goodrick, J. Brenner, Florida's fire management information system, in: Proceedings of the Joint Fire Science Conference and Workshop, 1517, University of Idaho Press, Boise, ID, USA, 1999, June.
[22] I. Keramitsoglou, C.T. Kiranoudis, H. Sarimvels, N. Sifakis, A multidisciplinary decision support system for forest fire crisis management: DSS for forest fire crisis management, Environ. Manag. 33 (2004) 212–225.
[23] A. Ilmavirta, The use of GIS-system in catastrophe and emergency management in Finnish municipalities, Comput. Environ. Urban Syst. 19 (3) (1995) 171–178.
[24] S. Botton, F. Duquenne, GPS, Location and Navigation, [M] Edition Hermes, Paris, France, 1997.
[25] S. Sauvagnargues, G. Dusserre, J.C. Poppi, R. Barre, Geographical Information Systems applied to security services, International Journal of GIS and spatial analysis 7 (1997) 353–371.
[26] H. Adab, K.D. Kanniah, K. Solaimani, Modeling forest fire risk in the northeast of Iran using remote sensing and GIS techniques, Nat. Hazards 65 (2013) 1723–1743.
[27] E. Chuvieco, R.G. Congalton, Application of remote sensing and geographic information systems to forest fire hazard mapping, Rem. Sens. Environ. 29 (2) (1989) 147–159.
[28] E. Chuvieco, J. Salas, Mapping the spatial distribution of forest fire danger using GIS, Int. J. Geogr. Inf. Sci. 10 (3) (1996) 333–345.
[29] B. Pradhan, M.D.H.B. Suliman, M.A.B. Awang, Forest fire susceptibility and risk mapping using remote sensing and geographical information systems (GIS), Disaster Prev. Manag. 16 (3) (2007) 344–352.
[30] I. Setiawan, A.R. Mahmud, S. Mansor, A.R. Mohamed Shariff, A.A. Nuruddin, GIS-grid-based and multi-criteria analysis for identifying and mapping peat swamp forest fire hazard in Pahang, Malaysia, Disaster Prev. Manag. 13 (5) (2004) 379–386.
[31] M. Ranagalage, M.H.J.P. Gunarathna, T.D. Surasinghe, D. Dissanayake, M. Simwanda, Y. Murayama, A. Sathurusinghe, Multi-decadal forest-cover dynamics in the tropical realm: past trends and policy insights for forest conservation in dry zone of Sri Lanka, Forests 11 (8) (2020) 836.
[32] K.U.J. Sandamali, K.A.M. Chathuranga, Quantification of burned severity of the forest fire using Sentinel-2 remote sensing images: a case study in the Ella Sri Lanka, Res. Rev.: J. Environ. Sci. 3 (2) (2021) 1–12.
[33] B.M.R.L. Basnayake, D.A.M. De Silva, S.K. Gunatiliake, R.R.M. Sandamith, I. Wickramarathna, Co-management initiatives in bush fire management—a case of Belihuloya Mountain range, Sri Lanka, in: Multi-Hazard Early Warning and Disaster Risks, Springer International Publishing, 2021, pp. 443–455.
[34] FAO, Global Forest Resources Assessment 2010: Country Report – Sri Lanka, FAO Forestry Department, Rome, 2010. Available at: http://www.fao.org/docrep/013/al632E/al632e.pdf, 2023-05- 14.
[35] R.K. Makumbura, J. Samarasinghe, U. Rathnayake, Multidecadal Land Use Patterns and Land Surface Temperature Variation in Sri Lanka, Applied and Environmental Soil Science, 2022, 2022.
[36] FAO, Brief on National Forest Inventory NFI 2007: Country Report – Sri Lanka, FAO Forestry Department, Rome, 2007. Available at: https://www.fao.org/forestry/18240-0f872ca779f7008c60a5af4f255ae3ea5.pdf, 2023-05- 14.
[37] I.M. Chathuranika, M.B. Gunathilake, H. Md Azamathulla, U. Rathnayake, Evaluation of future streamflow in the upper part of the Nilwala River Basin (Sri Lanka) under climate change, Hydrology 9 (3) (2022) 48, https://doi.org/10.3390/hydrology9030048.
[38] H. Abedi Gheshlaghi, Using GIS to develop a model for forest fire risk mapping, Journal of the Indian Society of Remote Sensing 47 (7) (2019) 1173–1185.
[39] A. Parajuli, A.P. Gautam, S.P. Sharma, K.B. Bhujel, G. Sharma, P.B. Thapa, S. Poudel, Forest fire risk mapping using GIS and remote sensing in two major landscapes of Nepal, Geomatics, Nat. Hazards Risk 11 (1) (2020) 2569–2586.
[40] J.D. Kushla, W.J. Ripple, The role of terrain in a fire mosaic of a temperate coniferous forest, For. Ecol. Manag. 95 (2) (1997) 97–107.
[41] J.R. Anderson, A Land Use and Land Cover Classification System for Use with Remote Sensor Data, 964, US Government Printing Office, 1976.
[42] T. Lillesand, R.W. Kiefer, J. Chipman, Remote Sensing and Image Interpretation, John Wiley & Sons, 2015.
[43] C. Schmidt, A. McCullum, Assessing the Accuracy of Land Cover Classifications, 2018.
[44] S.S. Rwanga, J.M. Ndambuki, Accuracy assessment of land use/land cover classification using remote sensing and GIS, Int. J. Geosci. 8 (4) (2017) 611.
[45] Landsat 8 science data users handbook, Land 8 (L8) (2019) data users handbook, https://prd-wret.s3.us-west-2.amazonaws.com/assets/palladium/production/atoms/files/. LSDS-1574_L8_Data_Users_Handbook-v5.0.pdf.

[46] D.A. Artis, W.H. Carnahan, Survey of emissivity variability in thermography of urban areas, Rem. Sens. Environ. 12 (4) (1982) 313–329.
[47] J.A. Sobrino, J.C. Jiménez-Muñoz, L. Paolini, Land surface temperature retrieval from LANDSAT TM 5, Rem. Sens. Environ. 90 (4) (2004) 434–440.
[48] J.A. Sobrino, V. Caselles, F. Becker, Significance of the remotely sensed thermal infrared measurements obtained over a citrus orchard, ISPRS J. Photogrammetry Remote Sens. 44 (6) (1990) 343–354.
[49] T.N. Carlson, D.A. Ripley, On the relation between NDVI, fractional vegetation cover, and leaf area index, Rem. Sens. Environ. 62 (3) (1997) 241–252.
[50] C.O. Justice, E. Vermote, J.R. Townshend, R. Defries, D.P. Roy, D.K. Hall, M. J. Barnsley, The Moderate Resolution Imaging Spectroradiometer (MODIS): land remote sensing for global change research, IEEE Trans. Geosci. Rem. Sens. 36 (4) (1998) 1228–1249.
[51] C.O. Justice, L. Giglio, S. Korontzi, J. Owens, J.T. Morisette, D. Roy, Y. Kaufman, The MODIS fire products, Rem. Sens. Environ. 83 (1–2) (2002) 244–262.
[52] L. Giglio, J. Descloitres, C.O. Justice, Y.J. Kaufman, An enhanced contextual fire detection algorithm for MODIS, Rem. Sens. Environ. 87 (2–3) (2003) 273–282.
[53] V. Tanpipat, K. Honda, P. Nuchaiya, MODIS hotspot validation over Thailand, Rem. Sens. 1 (4) (2009) 1043–1054.
[54] N. Serra-Sogas, P.D. O'Hara, R. Canessa, P. Keller, R. Pelot, Visualization of spatial patterns and temporal trends for aerial surveillance of illegal oil discharges in western Canadian marine waters, Mar. Pollut. Bull. 56 (5) (2008) 825–833.
[55] Z. Zhang, Z. Feng, H. Zhang, J. Zhao, S. Yu, W. Du, Spatial distribution of grassland fires at the regional scale based on the MODIS active fire products, Int. J. Wildland Fire 26 (3) (2017) 209–218.